Journal of Marine Systems, 1 (1991) 299–313
Elsevier Science Publishers B.V., Amsterdam

Predictability of the tropical Atlantic Ocean

James A. Carton and J. Shukla
Center for Ocean-Land-Atmosphere Interactions, Department of Meteorology, University of Maryland, College Park, MD 20742, U.S.A.

Received September 24, 1990; revised version accepted October 18, 1990

ABSTRACT

Carton, J.A. and Shukla, J., 1991. Predictability of the tropical Atlantic Ocean. J. Mar. Syst., 1: 299–313.

We have used a primitive equation multi-level model of the tropical Atlantic Ocean to calculate the time evolution of sea surface temperature and ocean circulation due to a prescribed surface stress forcing for a given year. We have then repeated the model integration starting from the same initial oceanic state as the first integration but with quite different surface stress forcing given by atmospheric observations from another year. We have examined the rate at which the differences between the two model-simulated ocean states grow with time and find that it takes only about three months for the differences to grow from zero to their saturation value. We have also examined the time growth of differences between two ocean model simulations for which the atmospheric forcing of surface stress was identical but the initial ocean states were quite different. In this case also, we find that it takes only about three months for the initial large differences to decay to their minimum value.

The results of these experiments lead to the following conclusions: (1) In the absence of accurate surface forcing, an accurate estimate of the ocean circulation at some initial time will lead to a reasonable estimate of circulation for only a few months. (2) Given accurate surface forcing, errors in the thermal and velocity structure of the ocean decrease rapidly within a few months. However some residual error will remain.

Introduction

Recent successful simulations of the tropical ocean circulation with multi-level high resolution ocean general circulation models have given some hope for the possibility of making forecasts of tropical sea surface temperature (*SST*) and ocean circulation (Philander and Seigel, 1985). These simulations have been carried out with the observed surface stress forcing and simple parameterizations of surface heat flux forcing. A reason for these successes is that the variability of tropical oceans is largely controlled by atmospheric forcing. Internal dynamical instabilities seem to play little, if any, role which implies that the state of the ocean at some time can be determined just by knowing the history of surface forcing. In the coupled ocean/atmosphere forecast problem the surface forcing will never be known ahead of time and therefore it will be useful to estimate the effects of incorrect surface forcing on the predictability of tropical *SST* and circulation. This paper is an attempt to estimate these effects.

During the past 20 years there have been numerous studies examining the classical predictability of atmospheric circulation (see Lorenz, 1965; Charney et al., 1966 and Shukla, 1985 for reviews) and it is understood that due to the nonlinearity and instability of atmospheric flows and imperfections of atmospheric models, small errors introduced in the definitions of the initial state of the atmosphere grow and make the forecasts useless after 2–3 weeks. Errors in the boundary conditions for the atmosphere (viz. *SST* at the lower boundary and solar forcing at the upper boundary) do not affect the nature of the error growth in any significant way. This is prim-

0924-7963/91/$03.50

arily so because surface boundary forcing changes slowly compared to the time-scales of atmospheric fluctuations.

The question of predictability of tropical *SST* and ocean circulation differs from that of atmospheric circulation in a very important aspect. Atmospheric fluctuations are in fact the forcing for oceanic circulation and therefore, unlike the question of atmospheric predictability where the the primary concern is the errors in the initial conditions and the model, for investigating the predictability of the tropical ocean one must also consider the effects of errors in boundary conditions. In fact it will be seen that this is an important factor limiting the predictability of the tropical ocean circulation. In contrast to the atmosphere, if perfect surface forcing were available, the ocean's response becomes largely predictable.

Philander et al. (1987) have argued convincingly that the influence of errors in initial conditions on the evolution of the circulation in a prognostic ocean model is partly a matter of dynamic adjustment. In dynamic adjustment various low frequency waves set up pressure gradients to balance the wind stress and so reduce the acceleration of the currents. According to this view the equatorial Atlantic will lose memory of its initial state in approximately the time it takes a low mode Kelvin wave to travel eastward along the equator from shore to shore (one month for a wave travelling at 2.5 m/s) and for a low mode Rossby wave to return ($\approx$ three months). However the speeds of waves involved in dynamic adjustment depend on the space and time scales of the wind field and decrease at higher latitudes, so the time during which adjustment occurs may vary. In the Pacific Ocean this mechanism is complicated by the possibility of rapidly growing coupled ocean/atmosphere instabilities which would make the ocean sensitive to its initial state (eg. Philander et al., 1984; Gill, 1985). However there isn't yet evidence for strong coupled instabilities in the Atlantic.

We note that an alternative mechanism for predictability of the coupled system has been proposed by Cane and Zebiak in a series of papers (Cane et al., 1986; Cane and Zebiak, 1987; Zebiak and Cane, 1987; Zebiak, 1989). They argue that it is the longer time-scales associated with the build-up of heat in the equatorial ocean which gives rise to El Niño. Irregular, but predictable exchanges of heat occur between the ocean and atmosphere so Pacific Ocean changes should be predictable on time-scales of a year or more. However Goswami and Shukla (1990) in examining the same model, have concluded that this mechanism, at most, accounts for only a fraction of the predictability of the system and that the system memory is lost as the ocean responds to errors in the wind field and through the growth of coupled ocean/atmosphere instabilities (also discussed by Philander and Lau, 1988).

In this paper we follow the classical approach pioneered for atmospheric predictability studies in which identical twin experiments are carried out either by changing the initial conditions or boundary conditions. Since this is, to our knowledge, the first study to consider both types of experiments, we have chosen to examine the influence of very large changes in the initial and boundary conditions. In the future such investigations can be refined by introducing more realistic perturbations in the initial and boundary conditions.

If accurate analyses of ocean circulation were available, as they are of the atmosphere we could use them to provide initial conditions and verification. In the absence of oceanic analyses we rely on a multi-year integration of the ocean model which we regard as the "true ocean circulation". The winds of the tropical Atlantic are highly seasonal, much more seasonal than in the Pacific, and so the oceanic thermal fields for January for several years forms a set of similar, but not identical, conditions which we will use for initial condition error experiments.

The multi-level primitive equation model used for the numerical experiments has been described in the next section. The subsection gives a brief description of the tropical Atlantic circulation as seen in the numerical simulation. We have conducted two sets of experiments:

– *Errors in boundary conditions*: we start with identical initial ocean states, but force the model with two quite different surface forcing functions

and examine the rate at which the solutions diverge. The limit of this experiment has been examined by a number of authors, (Inoue and O'Brien, 1984; Latif, 1987; Leetmaa and Ji, 1990; McPhaden et al., 1989 and comprehensively by Harrison et al., 1989) by comparing differences in the response of the Pacific Ocean to different wind analyses. Of these studies only Inoue and O'Brien examined the rate of divergence, and only for one case in a simplified ocean model. Our results are described in the third section.

– *Errors in initial conditions*: we use the identical atmospheric forcing but start pairs of simulations with quite different initial conditions. The second set of experiments are similar to the one reported in Philander et al. (1987)—the only difference being that they were mainly interested in the adjustment time whereas we present the growth rate of area averaged errors in attempt to determine the deterministic predictability of tropical ocean circulation. These results are described in the fourth section. The fifth section gives a summary and discussion of results.

The model

The primitive equation model used in these calculations is that of Philander and Pacanowski (1986). Horizontal friction and diffusion are assumed to be harmonic with a diffusion coefficient of 2×10^7 cm^2/s. Vertical friction and diffusion have the same Richardson number dependent formulation as in Pacanowski and Philander (1981), allowing mixing to increase in high shear regions such as the undercurrent.

The model domain extends from 30°S to 50°N with $1° \times \frac{1}{3}°$ resolution equatorward of 10° and coarser resolution at high latitudes (Fig. 1). The vertical differencing is carried out on 27 level surfaces, with 10 m spacing in the upper 100 m. Realistic basin geometry and topography are included. The first model gridpoint is at 5 m depth, but for convenience the temperature is assumed to be uniform for the upper 5 m. The meridional boundary conditions specify that the model temperature and salinity fields relax to seasonal climatological conditions at 30°S and 50°N. The seasonal climatology is that of Levitus (1982).

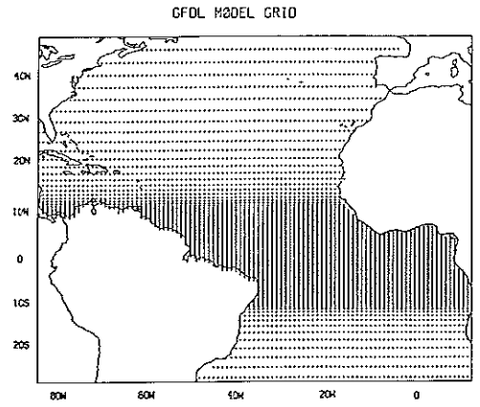

Fig. 1. Model grid.

The model is forced by the observed wind stress data set of V. Cardonne (pers. commun., 1986), based on the European Centre for Medium Range Weather Forecasts (ECMWF) wind product with the wind directions corrected to be consistent with ship wind observations. The winds are linearly interpolated from the monthly average at each time step. Surface heating due to incident solar radiation is assumed to have a constant value corresponding to its climatological average. Sensible and latent heating are estimated from a bulk formula which depends on the air–sea temperature contrast where climatological seasonal air temperature is specified (described in Philander and Pacanowski, 1986).

We estimate the damping time-scale by determining the time required for a uniform temperature mixed layer to come into equilibrium when the ocean is initially 29°C and the atmosphere is 28°C. For a 150 m deep mixed layer 100 days is required for the change in ocean temperature from its initial value to reach 90% of its final value. For a 100 m deep mixed layer this time-scale reduces to 75 days. Experiments have been conducted to examine the impact of an alternative, noninteractive heat flux formulation in which the ocean temperature is assumed to be a uniform 27°C in the evaporation calculation instead of being the surface temperature predicted by the model. The effect of changing the heat flux formulation is discussed in the third section. Some repetition of the experiments described here with this alternative heat flux formulation gives results similar to those presented.

In a separate study we have carried out a detailed comparison of the model integration with simultaneous direct observations of surface and subsurface temperature and velocity (Carton and Hackert, 1990). We have found that the seasonal changes produced by the model are qualitatively correct although of somewhat reduced amplitude. Interannual variations are also somewhat weak due to reduced interannual variability in the wind field and the model does contain systematic (time mean) errors of up to several degrees at thermocline depths due to misplacement and spreading of the thermocline. However, because the different model integrations compared in this study have similar systematic errors, we believe that they do not significantly influence the differences between model integrations.

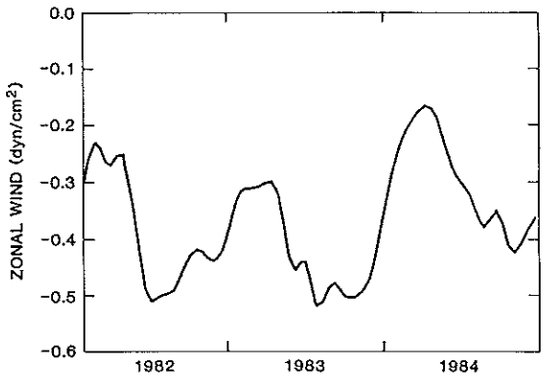

Fig. 3. Zonal wind stress over the equatorial ocean (2°S–2°N, 45°W–15°E) as a function of time.

Seasonal circulation

The tropical Atlantic Ocean has a strong seasonal cycle, driven by seasonal changes in the wind field. During the boreal late winter and spring the trade winds along the equator weaken and the eastward flowing North Equatorial Counter Current disappears. Along the coast of Brazil the North Brazil Current extends northward carrying water into the Guiana Current. Warm water is

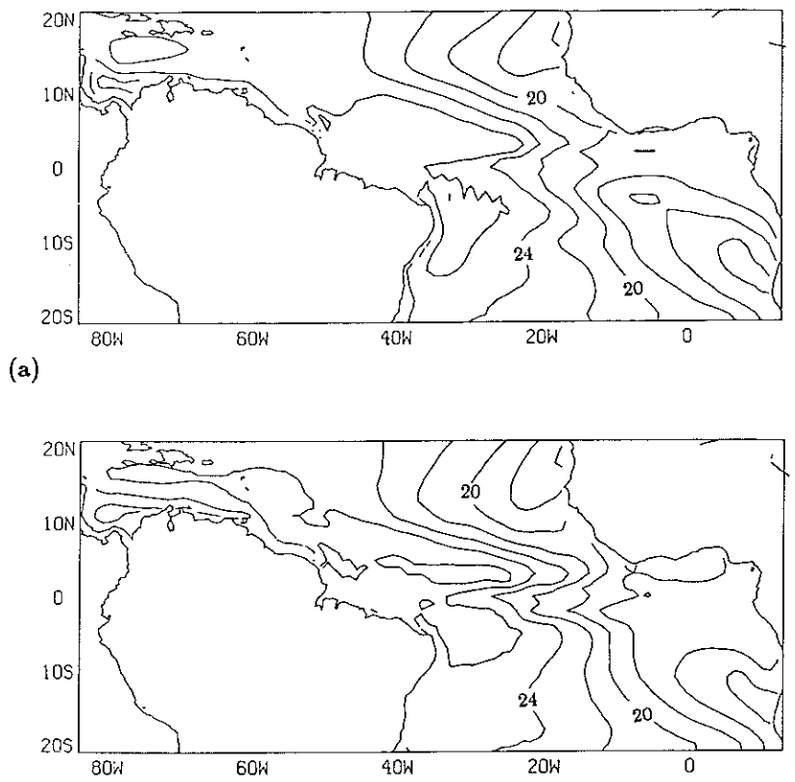

Fig. 2. Temperature at 55 m for the control run. (a) January, 1983 and (b) July, 1983. The contour interval is 2°C.

confined to the west with cold water to the east, particularly poleward of 10°. These features are evident in the model-derived thermal fields (Fig. 2a,b).

As the year progresses the convergence zone in the wind field shifts northward and the Counter Current returns, in association with a deepening of the thermocline north of the equator, where 55 m temperatures reach 29° C. The thermocline rises in the Gulf of Guinea in response to wind-induced upwelling. This steepens the slope of the thermocline and increases the zonal temperature gradient at 55 m. Surface temperature (not shown) also has a significant seasonal cycle. During the winter warm surface temperatures appear in the northern Gulf of Guinea. By summer the cool anomaly

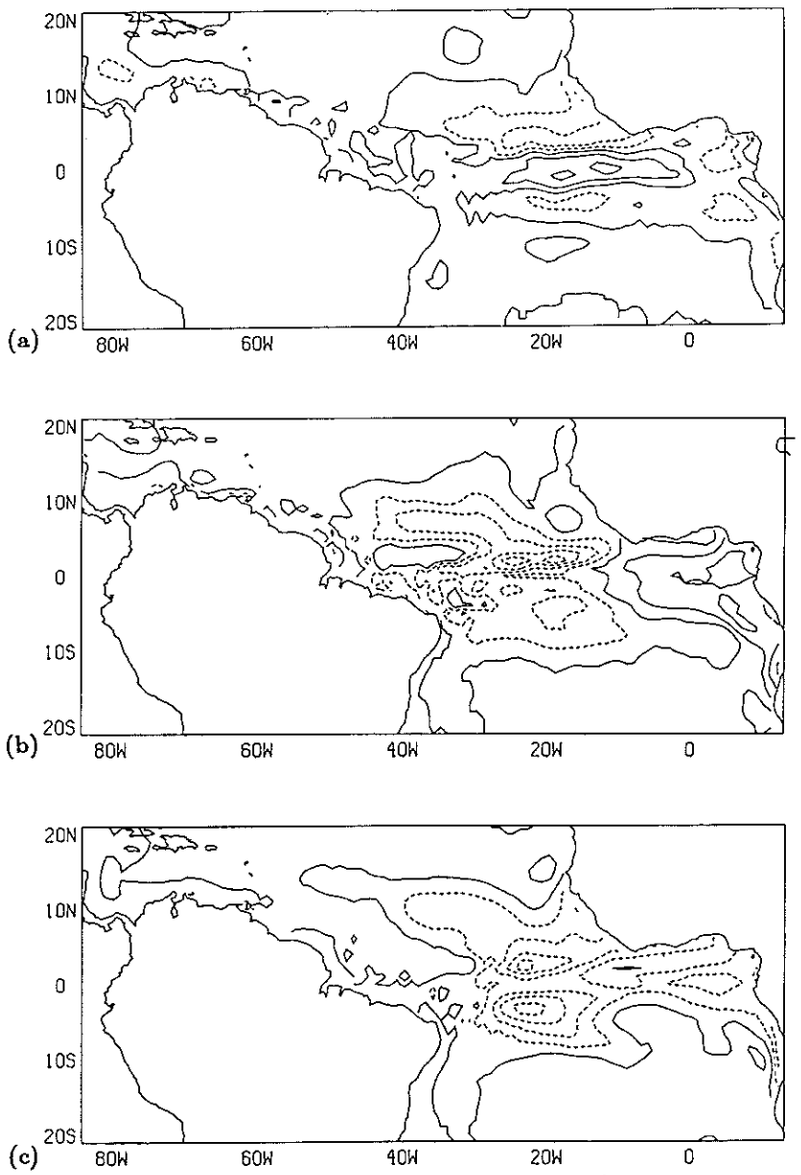

Fig. 4. Spatial distribution of temperature differences at 55 m (a) differences between January, 1984 and January, 1983, (b) differences between July, 1984 and July, 1983, and (c) differences between January, 1985 and January, 1983. Contour interval is Dashed lines indicate negative differences.

along the equator intensifies and the warm region north of the equator expands westward, increasing the north–south temperature gradient along the equator.

In addition to the predominant seasonal cycle, the tropical Atlantic does show some interannual changes. During much of 1983 the trade winds in the western tropical Atlantic were anomalously intense causing the average zonal winds along the equator to be stronger than normal. As the trade winds relaxed in early 1984, the convergence zone in the wind field was shifted unusually far southward and the zonal component of the trade wind stress near the equator dropped below 0.2 dynes/cm^2 (Fig. 3). In response, the temperature fields for January, 1984 show a strong warming of the eastern equatorial region compared to 1983 (temperature differences are shown in Fig. 4a) (Philander, 1986). This warming is associated with a deepening of the thermocline similar to that observed along a meridional transect at 4° W in early 1984 (Houghton and Colin, 1986). North and south of the equator in the east, the cold intrusions intensify, with 55 meter water reaching temperatures of 14° C in the tropics. As this cold water approaches the equator it causes a strong meridional temperature contrast. In July the eastern Gulf of Guinea is anomalously warm, while the central basin shows cooler temperatures. The temperature fields in January, 1985 are anomalously cold throughout the equatorial zone, as indicated by the temperature difference from January, 1983 shown in Fig. 4c. Weakly warmer temperatures prevail poleward of 10°.

Errors in boundary conditions

To provide the initial conditions for the identical twin experiments, and for verification, we use a multi-year control simulation (kindly provided by G. Philander). This simulation has been carried out by forcing the same numerical model with identical parameters as used in this study, with observed winds from January 1982 to January 1985. The initial conditions for the control simulation are provided by the model-simulated climatological January conditions of temperature and salinity (described in Philander and Pacanowski, 1986). Our identical twin experiments use the second two years of the simulation.

TABLE 1

Numerical simulations of tropical Atlantic circulation during 1982–1985. Initial conditions are provided by the control simulation except as noted. The starting date of the surface wind forcing varies between simulations

Simulation designation	Date of density initial conditions [1]	Beginning date of forcing	Duration (months)
Control	1-15-82 [2]	1-15-82	36
A	1-15-83	1-15-83	7
B	1-15-84	1-15-83	7
C	1-15-85	1-15-83	4
D	1-15-83 [3]	1-15-83	4
E	7-15-83	7-15-83	4
F	7-15-84	7-15-83	4
G	1-15-83	1-15-84	7
H	1-15-83	1-15-82	4
I	1-15-84	1-15-84	4
J	1-15-83	1-15-83 [4]	4

[1] Initial velocity fields are zeroed.
[2] Initial density fields are obtained by integrating the model with climatological forcing for several annual cycles.
[3] Temperature fields corrected by objective analysis.
[4] Heat flux modified to use specified climatological latent heating instead of interactive latent heating.

In the first set of experiments we compare simulations begun with identical initial conditions, but forced by winds from different years. In these experiments we examine the extreme hypothesis that the initial state of the ocean can be determined accurately, but that the surface forcing is known only crudely. There are three independent pairs of simulations which allow us to examine this hypothesis: *A–G*, *A–H*, *B–I*. We use this two letter designation to describe the pairs with each letter representing one of the simulations listed in Table 1. The simulations are defined as follows:

Simulations A, G and H. In these simulations (listed in Table 1) initial conditions of temperature and salinity are obtained from the control simulation at January 15, 1983. Thus the initial conditions for the three simulations are identical. The surface forcing is linearly interpolated at each time step from successive monthly averaged winds and surface temperature, as described in the second section. In simulation *A* the forcing begins on

January 15, 1983 for *G* it begins on January 15, 1984, and for *H* it begins on January 15, 1982.

Simulations B and I. In these simulations the initial conditions are obtained from the control simulation on January 15, 1984. The forcing begins on January 15, 1983 for *B* and January 15, 1984 for *I*. For *B*, as well as for *G* and *H* the winds are considerably out of balance with the model initial conditions and so the model undergoes a period of adjustment.

Each experiment consists of a pair of simulations which, since they have the same initial conditions, have an initial difference of zero. The difference grows as the different winds force changes in the circulation. We interpret these *differences* between the pairs of simulations as *errors* which are introduced into the model by inaccurate forcing, the inaccuracies being the difference between the two forcing fields. We use a root mean square (*RMS*) estimate to characterize the behavior of the errors for several different parameters as a function of integration time. For the quantity χ at level z_0, for simulations i and j, the *RMS* error integrated over an area $\iint da$ is defined as

$$RMS_{\chi_i,\chi_j}(t, z_0) = \frac{\left[\iint [\chi_i(t, z_0) - \chi_j(t, z_0)]^2 \, da\right]^{1/2}}{\left(\iint da\right)^{1/2}}. \quad (1)$$

For the discussion below unless otherwise specified $\iint da$ will include all the oceanic area from 15°S–15°N, 80°W–15°E.

The initial growth rate for *SST* error is 0.4°C/month (Fig. 5). The low errors of *A–H* after three months reflect the similarities between 1982 and 1983 winds. The largest errors are obtained when comparing simulations forced by the 1983 and 1984 winds because of the strong differences between these years. To obtain an estimate of the average error growth, we average the three *RMS* error curves of Fig. 5. For the average error this rate of growth (0.4°C/month) is maintained for two months, after which the error levels out at 0.9°C. The standard deviation of the growth curves shows that the estimate of error growth is only approximate due to the limited number of

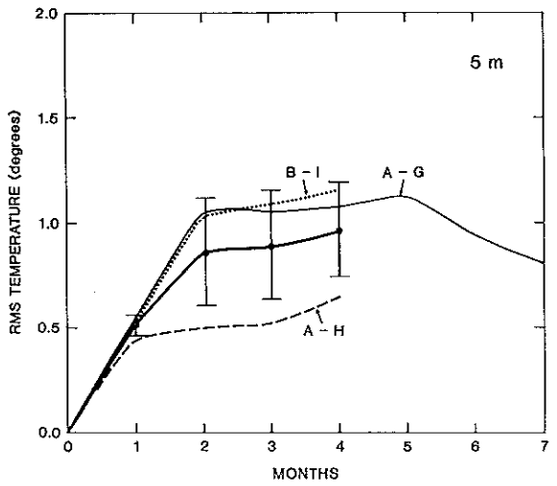

Fig. 5. *RMS* difference between surface temperature simulations averaged between 15°S–15°N as a function of integration time, computed from eqn. (1). The simulations are listed in Table 1 and indicated by upper case letters. The three pairs which are forced with differing winds but have identical initial conditions, are described in the text. The average of the individual curves is bold. The vertical bars show one standard deviation of the estimates. The saturation error estimated from the model simulations is 1.1°C.

simulations. The deeper temperature levels (Figs. 6a,b) show a memory time which is similar to that of *SST*. The zonal velocity errors (Figs. 6c,d) exceed 10 cm/s in the surface and greater than 6 cm/s at 50 m after a month. After this time the errors remain relatively constant.

After integrating for a long time, the errors can be expected to become as large as the differences between any two surface temperature analyses for the same month of randomly chosen years. In numerical weather prediction this limit is known as the saturation error and can be calculated from historical analyses of weather. For the ocean the only variable which is available for many years is *SST*. Servain et al. (1987) has produced a many year analysis of monthly *SST* for the Atlantic based on ship observations. The root mean square of the temperature differences in all months from year to year in the region 15°S–15°N from Servain's analysis is 1.96°C. The difference between this number and the saturation error computed from the simulations indicates that the model has significantly less surface temperature variability ($\approx$ 1.1°C) than is observed. We believe

the lowered variability is partly due to the climatological heat flux parameterization, but the reduced variance of the monthly averaged winds may also be responsible. Although in this study we mainly consider the effect of errors in the surface winds, several experiments were conducted to examine the importance of errors in the surface heating. In one experiment listed as *J* in Table 1, the heat flux described above was modified, with the usual formulation of latent heating, which varies with simulated sea surface temperature, replaced with specified climatological seasonal latent heating derived from the Comprehensive Ocean–Atmosphere Data Set (Oberhuber, 1988). The incident solar radiation had to be increased somewhat in order to make the simulated *SST*'s reasonable in this experiment. Figure 7 shows the *RMS* differences between *J* and a simulation with the same initial conditions and winds (*A*). *SST* underwent a rapid change which was as large as the changes resulting from differing wind stresses, but this change was primarily nearsurface and occured

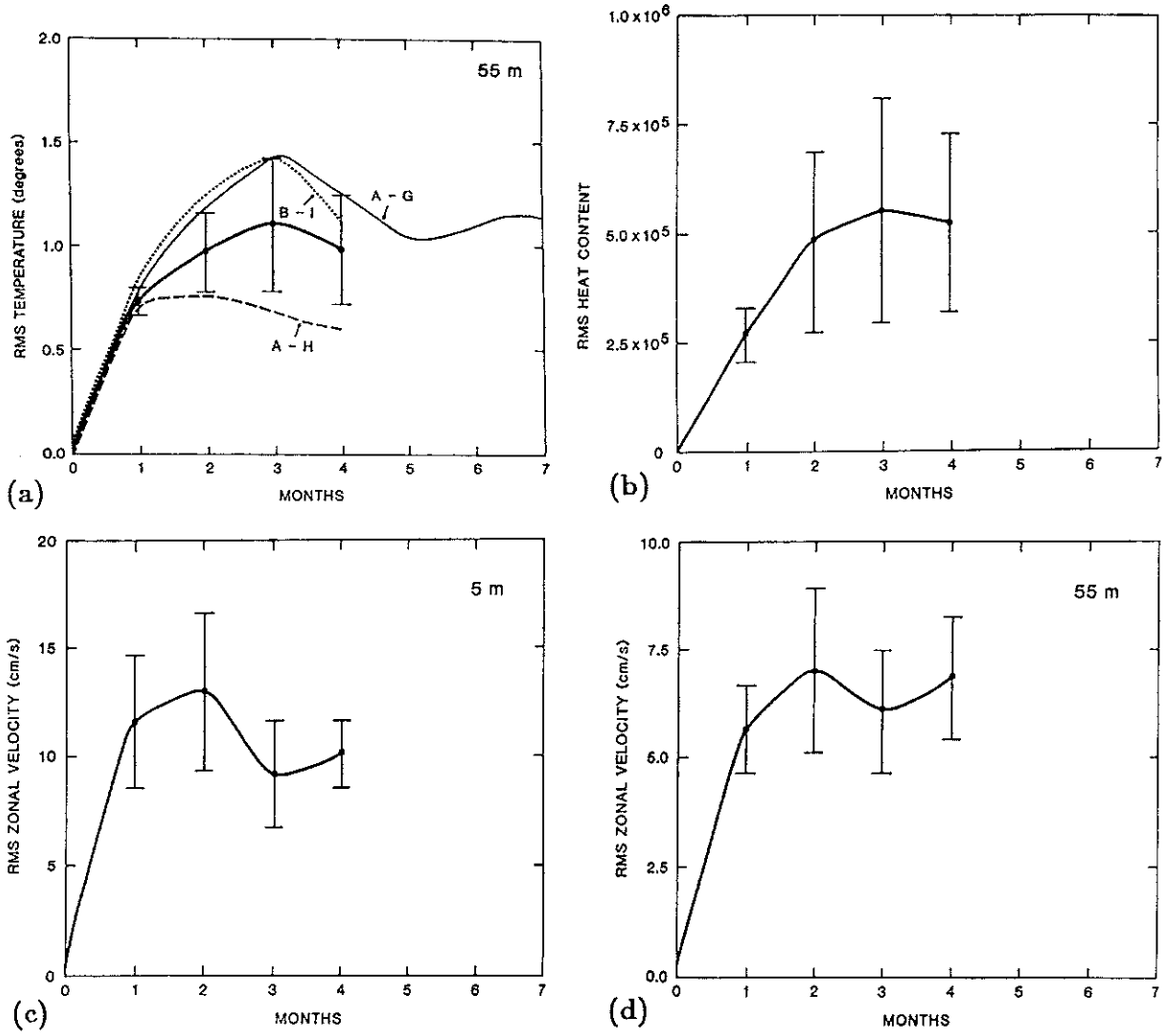

Fig. 6. Average *RMS* differences as a function of integration time for the pairs of simulations shown in Fig. 5. (a) 55 m temperature (individual curves included), (b) heat content, (c) surface zonal velocity and (d) 55 m zonal velocity. Heat content is defined as $\int_{-300\text{m}}^{0\text{m}} C_p T \, dz$, where $C_p = 3.99 \times 10^6$ Jm^{-3}°C^{-1}. Units are J/cm^2. Vertical bars show ± one standard deviation of the estimates.

over a longer timescale. Below the surface changing the surface heating had little impact in four months (compare the solid and dashed curves).

Averaging the errors with latitude masks some latitudinal dependence. The error growth of surface temperature is more rapid away from the equator, where surface temperature changes are mostly a function of local heating and storage, than in the equatorial band where advection is important (compare Fig. 8a,b). At 55 m the error growth of temperature is influenced by dynamic adjustment of the thermal structure. This occurs more rapidly in the equatorial zone than further north (compare Fig. 8c,d). As shown in the following section, both at surface and subsurface levels the saturation error is greater nearer the equator in the region of strong currents.

Errors in initial conditions

In the second set of experiments we compare simulations forced with identical winds, but begun with initial conditions from the same month of different years. In these experiments we examine the extreme hypothesis that the wind forcing can be determined accurately, through the use of a satellite scatterometer for example, but that the initial state of the ocean can be known only crudely due to limited subsurface data. We have five pairs of simulations which satisfy these conditions *A–B*, *A–C*, *A–D*, *E–F* and *G–I*. Each of these pairs is four months long except *A–B* which is extended to seven months. Other pairs can be formed but will not be independent of these.

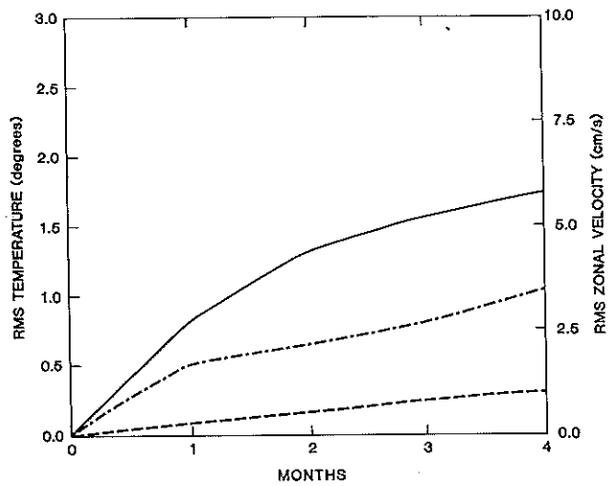

Fig. 7. *RMS* difference as a function of integration time for a pair of simulations *A* and *J* which have identical initial conditions and wind forcing. The simulations differ only in the specification of surface heat flux, with *A* having the usual interactive heat flux described in second section and *J* having specified climatological latent heating. Surface temperature (solid), 55 m temperature (dashed) and surface zonal velocity (dotted).

Simulations A, B, C and D. In these experiments the wind forcing begins on January 15, 1983. The initial conditions for *A*, *B* and *C* are obtained from the control run at January 15 of 1983, 1984, and 1985 respectively.

For *D* the initial conditions and initial date of the surface forcing are both January 15, 1983, as in *A*. However the initial temperature field has been updated using actual surface and subsurface temperature observations from December, 1982 through February, 1983. In the updating procedure, which is described in Carton and Hackert (1989), the simulated temperature fields for January 15, 1983 from the control run are used as a first guess. At each of the 20 model levels between the surface and 484 m, the temperature field is corrected for the approximately 400 independent measurements of temperature, using a space–time objective analysis procedure.

The subsurface observations of temperature differ significantly from the model simulated fields. This means that the initial conditions for *D* are more different from the control January, 1983 temperature fields than the simulated January, 1984 or 1985 initial conditions are from the control January, 1983 fields. As noted above, a comprehensive analysis of the data assimilation errors is provided in Carton and Hackert (1990).

Simulations E and F. In this experiment the simulations are forced with winds beginning July 15, 1983, during a time of the year when the intertropical convergence zone is shifted northward. The initial conditions are obtained from the control run from July 15, 1983 and 1984 respectively.

Simulations G and I. In this experiment the winds begin January 15, 1984 and as before the initial conditions are obtained from the control run for January 15, 1983 and 1984 respectively.

The *SST* error curves are shown in Fig. 9 as a function of integration time for all five simulation pairs. The pair containing *D*, the updated field, has the largest initial error, while the simulation pairs beginning with January 15, 1983 and 1984 fields (*A–B* and *G–I*) have the smallest initial error. The initial rate of error decay varies substantially among the simulation pairs. The simulations which were begun in July (*E–F*) maintain the largest error after four months (0.5 °C).

The average error has been computed as in the first experiments. The error is initially 0.8 °C, slightly less than the temperature error of 1.1 °C estimated from the initial conditions from the first set of experiments. The average error reduces within two months by more than a factor of two to 0.3 °C. The rapid decrease in errors within two months is consistent with a dynamic adjustment which rapidly redistributes density anomalies longitudinally. However, the meridional adjustment occurs more slowly. The residual error after four months results from changes in the total amount of heat in the tropics, which is determined by the balances of surface heating, storage and

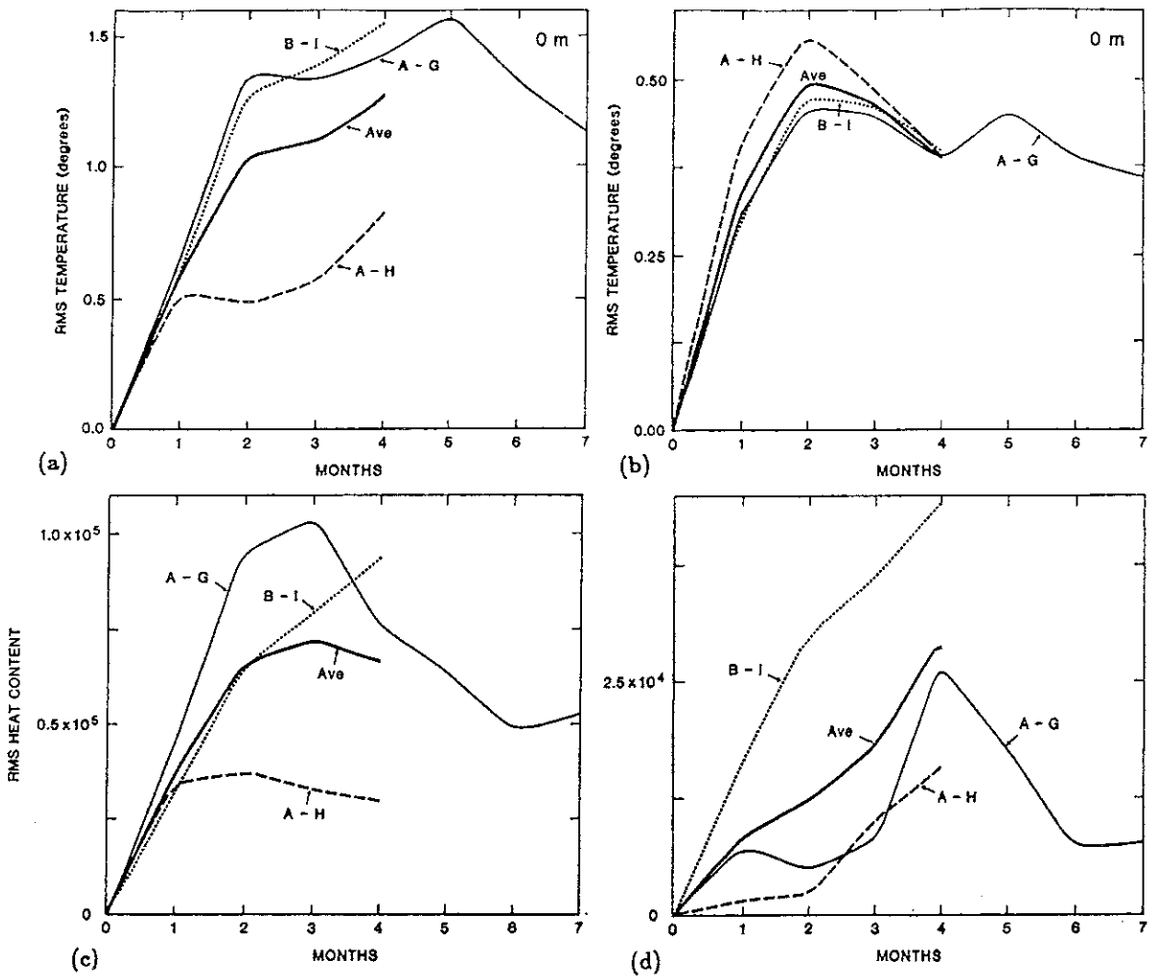

Fig. 8. *RMS* differences as a function of integration time zonally averaged in two latitude bands: an equatorial band 5 °S–8 °N and a northern band 8 °N–15 °N. (a) Surface temperature in the equatorial band, (b) surface temperature in the northern band, (c) 55 m temperature in the equatorial band, (d) 55 m temperature in the northern band.

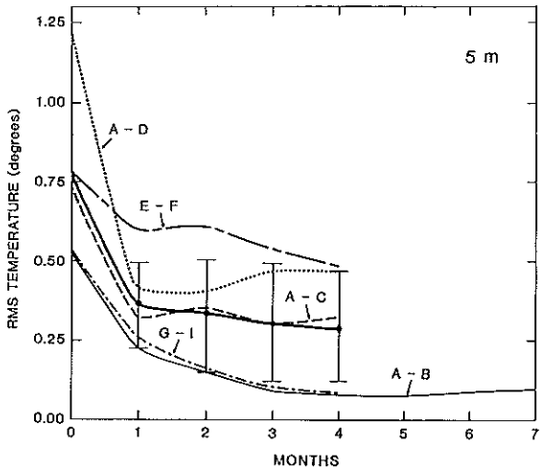

Fig. 9. difference between surface temperature simulations averaged between 15°S–15°N as a function of integration time, computed from eqn. (1). The simulations are listed in Table 1 and indicated by upper case letters. Five pairs of simulations are shown which are forced with identical winds but have differing initial conditions. The average of the five curves is bold. Vertical bars show one standard deviation about the average curve.

advection. Similar persistence of error can be seen in the 55 m temperature and heat content fields (Figs 10a,b).

Because the simulations are sampled once a month and the velocity fields are zero initially, the error curves in Fig. 10c,d only exist after one month of integration. The error is approximately constant for the second month of integration and then decays slowly through the third and fourth months. A convenient representation of the average error curves is given by an exponential expressing the rapid dynamical adjustment, plus a constant.

$$\overline{RMS_{X_i,X_j}(t)} \approx \left[\overline{RMS_{X_i,X_j}(t=0)} - \overline{RMS_{X_i,X_j}(t=\infty)}\right] \times e^{(-t/T_0)} + \overline{RMS_{X_i,X_j}(t=\infty)} \quad , \quad (2)$$

where $RMS_{X_i,X_j}(t=\infty)$ and decay time T_0 are estimated by a least squares fit to the average error curve. These numbers, given in Table 2, allow us to compare the characteristic adjustment time of different variables. In both temperature and velocity the adjustment occurs most rapidly in the upper ocean, and more rapidly in temperature than velocity. The residual error is larger at 55 m in temperature than at the surface, but is the same at both depths for velocity.

Even though the *magnitude* of the temperature error decreases by a factor of two in two months, the spatial distribution of the error is persistent. After two months of integration the $A-C$ 55 m temperature difference still shows a negative anomaly near the equator with minimum values in the central basin and positive differences poleward of 10°(compare Figs. 4b and 11a). The negative temperature anomaly in the central equatorial region has shifted eastward into the Gulf of Guinea, while the anomaly at 10°N has moved westward. Two months later the same pattern persists (Fig. 11b).

TABLE 2

Parameters estimated from the average error curves for the two sets of experiments

Quantity	$\overline{RMS(t=0)}$ *	$\overline{RMS(t=\infty)}$ *	Decay time T_0 * (months)	Growth rate ** (per month)
$T(z=5$ m)	0.78°C	0.3°	0.7	0.52°
$T(z=55$ m)	1.1°C	0.6°	2.5	0.75°
$\text{Heat}_{0/300}$	4.7×10^5 J/cm^2	2.0×10^4	1.0	2.8×10^5
$u(z=5$ m)	6.0 cm/s	2.0	4.1	12.0
$u(z=55$ m)	4.6 cm/s	2.3	5.5	5.8

* Estimated by fitting eqn. (2) to the average error curves in Figs. 9 and 10.
** Initial growth rate estimated from Figs. 5 and 6.

Summary and discussion

In the first set of experiments we compare simulations begun with identical initial conditions, but forced by winds from different years. For these experiments, the initial error is zero and grows to a saturation value in the course of about three months. By comparing these experiments we are able to show that a very accurate estimate of the density field of the ocean at an initial time will lead to a reasonable estimate of the circulation only for a few months. After that the fields will be corrupted by errors in the wind field. The saturation value of the errors are an upper bound on the errors due to erroneous winds. For 55 m temperature this is about 1.1°. Initially the error increases at a rate of 0.75 °C per month. This large rate has important implications for the design of data assimilation systems. If the wind field is inaccurate, then it will be necessary to resample the Atlantic Ocean every month or two in order to maintain a simulation of 55 m temperature within one degree, for example.

In our second set of experiments we compare numerical simulations of Atlantic circulation using initial conditions from different years, for example

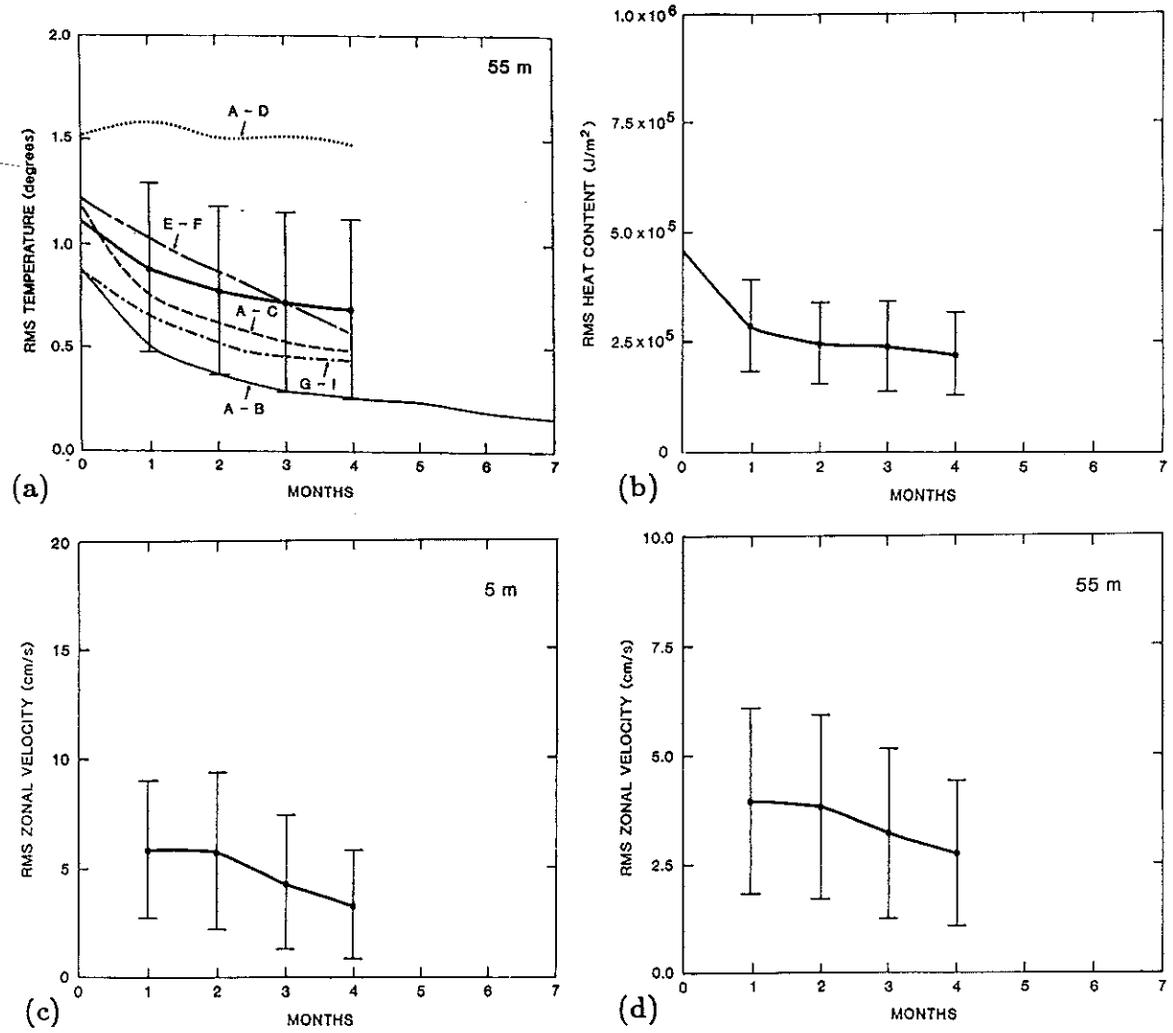

Fig. 10. Average *RMS* differences as a function of integration time for the pairs of simulations shown in Fig. 9. (a) 55 m temperature (individual curves included) (b) heat content, (c) surface zonal velocity and (d) 55 m zonal velocity. Heat content is defined as $\int_{-300}^{0m} {}_{m}C_{p}T\,dz$, where $C_p = 3.99 \times 10^6$ Jm^{-3}° C^{-1}. Units are J/cm^2. Vertical bars show ± one standard deviation of the estimates.

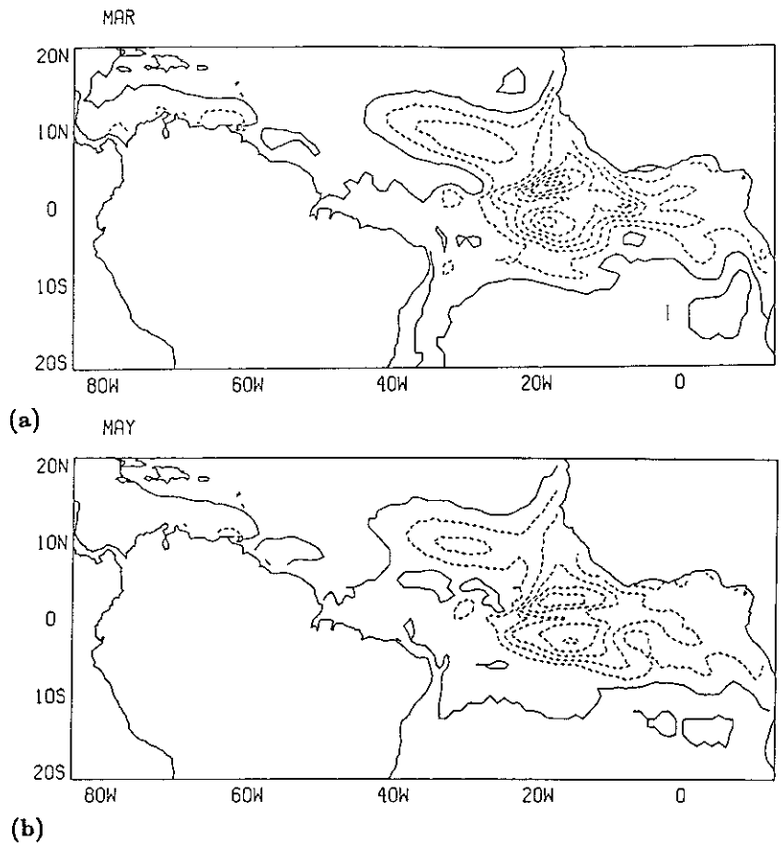

Fig. 11. Differences of 55 m temperature for simulations *A–C* after (a) two months and (b) four months of integration. Countour interval is 0.5° C.

from January, 1982 and January, 1983. The surface forcing however is the same for each pair of simulations. The initial differences gives a lower bound on our knowledge of the ocean circulation. These differences can be interpreted as the errors we could expect if we assumed that January conditions for any year were the same as January conditions for any other year. Much of this error is concentrated in a band of strong currents within a few degrees of the equator.

By comparing these pairs of simulations, we can show that errors in initial conditions will decrease substantially over several months. Surface temperature errors, for example, decrease by more than a factor of four over four months, to an average error of 0.3°. Similar decreases are found in heat content, and surface and thermocline speed.

A number of assumptions need to be made to obtain these results. First, we need to assume that the model provides a reasonable representation of the ocean. However, as noted in the discussion of Experiment *D*, the model does have significant large scale biases which may be due to incorrect specification of surface winds and heating. Parameterizations for friction and diffusion and the absence of some processes such as surface fresh water flux are additional potential sources of error. To interpret the results we either assume that the wind fields are very bad, as in our first set of experiments, or that the initial ocean states are bad as in our second. In reality, the winds are probably somewhere inbetween. The surface flux of heat is only very crudely represented and probably is a significant source of error for these simulations.

Even so these results have surprisingly strong implications for our ability to sample the oceans. If we assume that the surface winds will soon be

highly accurate because of the availability of scatterometry for example, and we assume that ocean models will soon be highly accurate, then we can expect from the results in Fig. 10d to be able to simulate the nearsurface currents to within a few centimeters per second by simply forcing an ocean model with observed forcing for several months. For direct observations of the ocean to improve on this estimate it would be necessary for the observations to be more precise than this. Furthermore, direct measurements of this accuracy would have to be made over significantly large areas for the information to directly improve our understanding of the large scale circulation.

These results provide a scientific basis for prediction of the coupled tropical ocean-atmosphere system, at least up to a season when rapidly growing instabilities do not dominate. In our first set of experiments we took a rather extreme view and assumed arbitrarily that atmospheric forcing has large error and still we found that it takes about three months for the ocean temperature to become completely unpredictable. Even in the real time operational ocean prediction system—whenever there will be one—the errors in the atmospheric forcing will be smaller than what we have chosen for this study and therefore our results should be viewed as a conservative estimate of the tropical ocean predictability.

Acknowledgements

Thanks are due to B. Huang for programming assistance and to the San Diego Super Computer Center for computer support. This research has been supported by the National Science Foundation OCE-86-10422 and OCE-90-00060 to J.A.C. and ATM-87-13567 to J.S.

References

Cane, M.A., Dolan, S.C. and Zebiak, S.E., 1986. Experimental forecasts of the 1982/83 El Niño. Nature, 321: 827–831.

Cane, M.A. and Zebiak, S., 1987. Prediction of El Niño events using a coupled model. In: H. Cattle (Editor), Atmospheric and Oceanic Variability. R. Meteorol. Soc., U.K., pp. 153–181.

Carton, J.A. and Hackert, E., 1989. Application of multivariate statistical objective analysis to the circulation in the tropical Atlantic Ocean, and its implications for data assimilation. Dyn. Atmos. Oceans, 13: 491–516.

Carton, J.A. and Hackert, E., 1990. Data assimilation applied to the temperature and circulation in the tropical Atlantic, 1983–4. J. Phys. Oceanogr., 20: 1150–1165.

Charney, J.G., Fleagle, R.G., Riehl, H., Lally, V.E. and Wark, D.Q., 1966. The feasibility of a global observation and analysis experiment. Bull. Meteorol. Soc., 47: 200–220.

Gill, A.E., 1985. Elements of coupled ocean–atmosphere models for the tropics. In: J.C.J. Nihoul (Editor), Coupled Ocean–Atmosphere Models. Elsevier, Amsterdam, pp. 303–326.

Goswami, B.N. and Shukla, J., 1990. Predictability of a coupled ocean–atmosphere model. submitted to J. Climate, 6: 1–21.

Harrison, D.E., Kessler, W.S. and Giese, B., 1989. Ocean circulation model hindcasts of the 1982–3 El Niño: Thermal variability along the ship-of-opportunity tracks. J. Phys. Oceanogr., 19: 397–418.

Houghton, R.W. and Colin, C., 1986. Thermal structure along 4° W in the Gulf of Guinea during 1983–1984. J. Geophys. Res., 91: 11727–11739.

Inoue, M., and O'Brien, J.J., 1984. A forecasting model for the onset of a major El Niño. Mon. Weather Rev., 112: 2326–2337.

Latif, M., 1987. Tropical ocean circulation experiments. J. Phys. Oceanogr., 17: 246–263.

Leetmaa, A. and Ji, M., 1990. Operational hindcasting of the tropical Pacific. Dyn. Atmos. Oceans, in press.

Levitus, S., 1982. Climatological Atlas of the world ocean. NOAA Prof. Pap. 13. U.S. Dep. Commerce, Rockville, Md., 174 pp.

Lorenz, E.N., 1965. A study of the predictability of a 28-variable atmospheric model. Tellus, 17: 321–333.

Lorenz, E.N., 1982. Atmospheric predictability experiments with a large numerical model. Tellus, 34: 505–513.

McPhaden, M.J., Busalacchi, A.J. and Picaut, J., 1989. Observations and wind-forced model simulations of the mean seasonal cycle in tropical Pacific sea surface topography. J. Geophys. Res., 93: 8131–8146.

Oberhuber, J.M., 1988. An atlas based on the "COADS" data set: the budgets of heat, buoyancy and turbulent kinetic energy at the surface of the global ocean. Max-Planck Inst. Meteorol. Hamburg. Rep. No. 15.

Pacanowski, R., and Philander, S.G.H., 1981. Parameterization of vertical mixing in numerical general circulation models of the tropical oceans. J. Phys. Oceanogr., 11: 1443–1451.

Philander, S.G.H., 1986. Unusual conditions in the tropical Atlantic Ocean in 1984. Nature, 122: 236–238.

Philander, S.G.H., Yamagata, T. and Pacanowski, R.C., 1984. Unstable air–sea interactions in the tropics. J. Atmos. Sci., 41: 604–613.

Philander, S.G.H. and Seigel, A.D., 1985. Simulation of El Niño of 1982–1983. In: J.C.J. Nihoul (Editor), Coupled Ocean Atmosphere Models. Elsevier, Amsterdam, pp. 517–541.

Philander, S.G.H. and Pacanowski, R.C., 1986. A model of the seasonal cycle of the tropical Atlantic Ocean. J. Geophys. Res., 91: 14192–14206.

Philander, S.G.H. and Lau, N.-C., 1988. Predictability of El Niño. In: M.E. Schlesinger (Editor), Physically-based Modelling and Simulation of Climate and Climate Change—Part II. Kluwer, Norwell, Mass., pp. 967–982.

Philander, S.G.H., Hurlin, W.J. and Pacanowski, R.C., 1987. Initial conditions for a general circulation model of the tropical oceans. J. Phys. Oceanogr., 17: 1986–2002.

Servain, J., Seva, M., Lukas, S. and Rougier, G., 1987. Climatic atlas of the tropical Atlantic wind stress and sea surface temperature, 1980–1984. Ocean–Air Interactions, 1: 109–182.

Shukla, J., 1985. Predictability. Adv. Geophys., 28b: 87–122.

Zebiak, S.E., 1989. Oceanic heat content variability and El Niño cycles. J. Phys. Oceanogr., 19: 475–486.

Zebiak, S.E. and Cane M.A., 1987. A model El Niño-Southern Oscillation. Mon. Weather Rev., 115: 2262–2273.